

Cold Nuclear Matter Effects on J/ψ Production in $p + A$, $d + Au$ and $A + A$ Collisions

R. Vogt

Nuclear Science Division, Lawrence Berkeley National Laboratory, Berkeley, CA
Physics Department, University of California, Davis, CA

In Collaboration with M. Leitch (Los Alamos) and C. Lourenco (CERN)

Outline

- **Baseline Nuclear Effects on Quarkonium Production**
 - Initial-State Shadowing
 - Final-State Absorption
- **Shadowing and Absorption in J/ψ and ψ' Production in $p + A$ at the SPS**
- **Comparison to RHIC $d + Au$ and $A + A$ Data**

Medium Effects Important in $p(\text{d})+A$ Interactions

Nuclear effects in fixed-target interactions

Parameterizing

$$\sigma_{pA} = \sigma_{pp} A^\alpha \quad \alpha(x_F, p_T)$$

For $\sqrt{S_{NN}} \leq 40$ GeV and $x_F > 0.25$, α decreases strongly with x_F – only low x_F effects probed by SPS and RHIC rapidity coverage

Consider two low x_F cold matter effects at colliders:

- Nuclear Shadowing — initial-state effect on the parton distributions affecting total rate, important as a function of y/x_F
- Absorption — final-state effect, after $c\bar{c}$ that forms the J/ψ has been produced, pair breaks up in matter due to interactions with nucleons

At high x_F , other mechanisms (energy loss, intrinsic charm) may be important but $x_F > 0.25$ corresponds to $y > 2.8$ at $\sqrt{S_{NN}} = 200$ GeV (larger y for higher \sqrt{S}) and do not appear in p_T -integrated y distributions

Nuclear Parton Distributions

Nuclear parton densities

$$F_i^A(x, Q^2, \vec{r}, z) = \rho_A(s) S^i(A, x, Q^2, \vec{r}, z) f_i^N(x, Q^2)$$
$$s = \sqrt{r^2 + z^2}$$
$$\rho_A(s) = \rho_0 \frac{1 + \omega(s/R_A)^2}{1 + \exp[(s - R_A)/d]}$$

With no nuclear modifications, $S^i(A, x, Q^2, \vec{r}, z) \equiv 1$

We use Eskola *et al.* (EKS98) and DeFlorian and Sassot (nDSg) parameterizations

Assume spatial dependence proportional to nuclear path length:

$$S_\rho^i(A, x, Q^2, \vec{r}, z) = 1 + N_\rho(S^i(A, x, Q^2) - 1) \frac{\int dz \rho_A(\vec{r}, z)}{\int dz \rho_A(0, z)}$$

Normalization: $(1/A) \int d^2r dz \rho_A(s) S_\rho^i \equiv S^i$. Larger than average modifications for $s = 0$. Nucleons like free protons when $s \gg R_A$.

Comparing Shadowing Parameterizations: x Dependence

EKS98 and nDSg available for all A

EKS98 has strong antishadowing at $x \sim 0.1$, nDSg has almost none

EKS98 and nDSg similar for $A = 208$ but nDSg weaker for smaller A

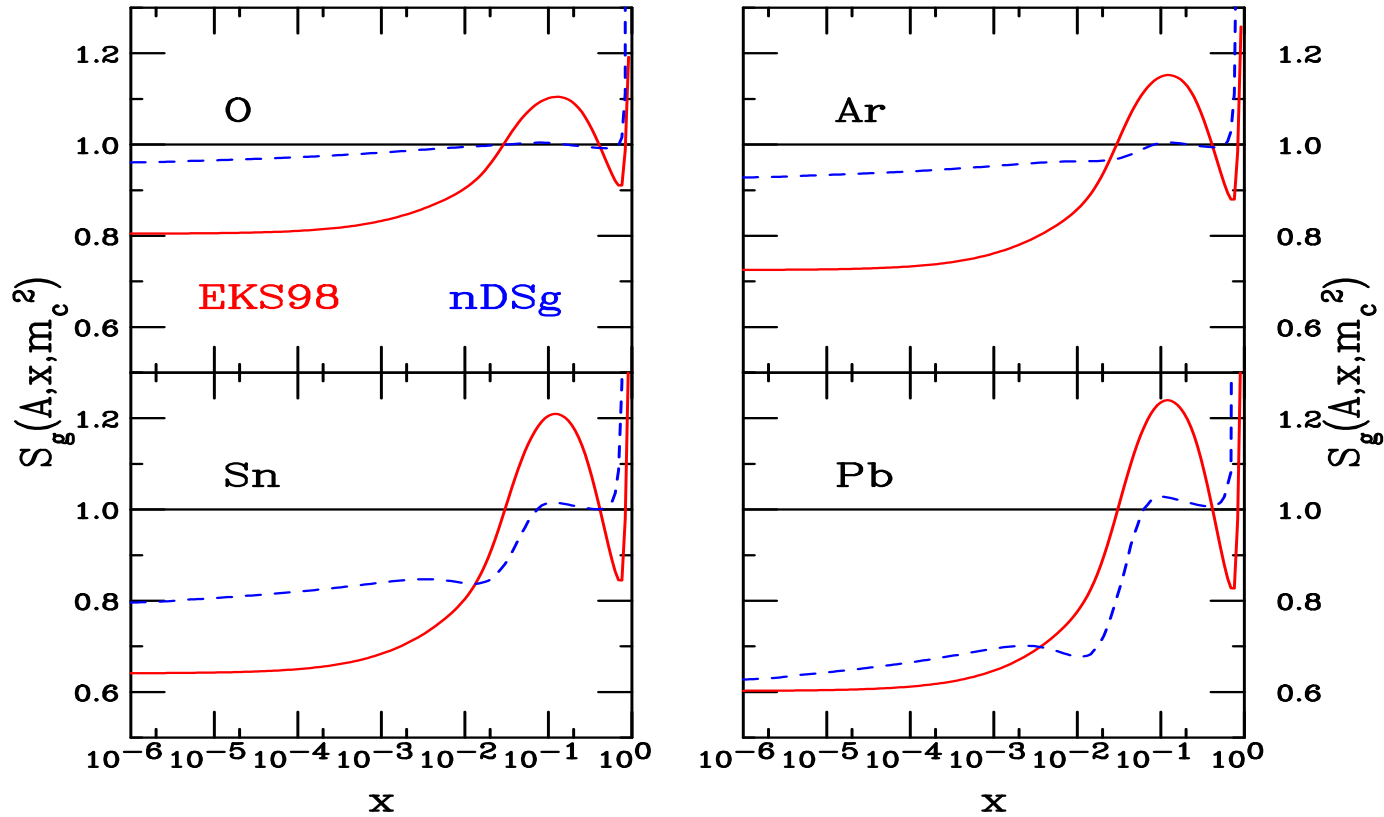


Figure 1: EKS98 (red) and nDSg (blue) gluon shadowing parameterizations for J/ψ production scales for $A = O, Ar, Sn$ and Pb .

Average x_2 as a Function of Energy and Rapidity

$\langle x_2 \rangle$ as a function of rapidity for $2 \rightarrow 2$ scattering (N.B. $\langle x_1 \rangle$ is mirror imagine of $\langle x_2 \rangle$)

Increasing \sqrt{S} broadens y range and decreases x_2

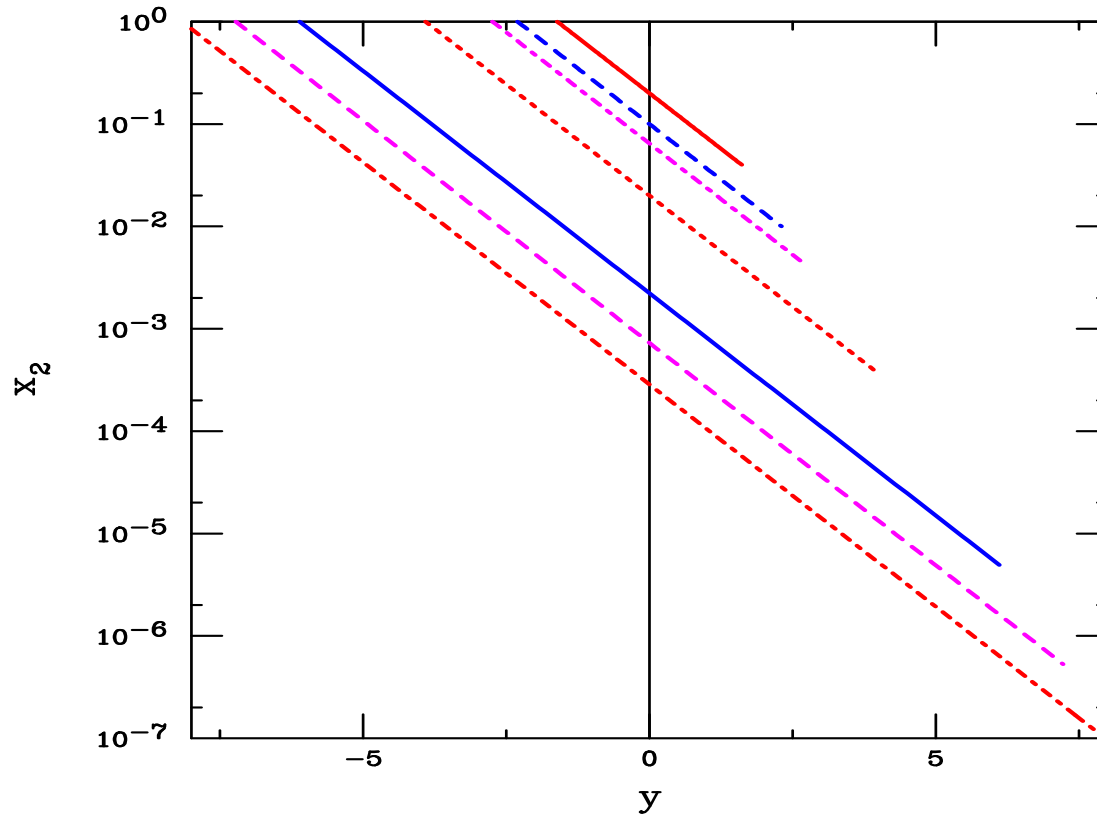


Figure 2: We give the average value of the nucleon momentum fraction, x_2 , in pp collisions as a function of rapidity for (top to bottom) $\sqrt{S_{NN}} = 20; 40; 62; 200; 1800; 5500$ and 14000 GeV.

Quarkonium Absorption by Nucleons

Woods-Saxon nuclear density profiles typically used

$$\begin{aligned}\sigma_{pA} &= \sigma_{pN} \int d^2b \int_{-\infty}^{\infty} dz \rho_A(b, z) S_A^{\text{abs}}(b) \\ &= \sigma_{pN} \int d^2b \int_{-\infty}^{\infty} dz \rho_A(b, z) \exp \left\{ - \int_z^{\infty} dz' \rho_A(b, z') \sigma_{\text{abs}}(z' - z) \right\}\end{aligned}$$

Note that if $\rho_A = \rho_0$, $\alpha = 1 - 9\sigma_{\text{abs}}/(16\pi r_0^2)$

The value of σ_{abs} depends on the parameterization of σ_{pA} – Glauber, hard sphere, A^α etc. (shown by NA50)

Initial-state shadowing not taken into account at SPS energies, increasing $\sqrt{S_{NN}}$ and rapidity range of measurement influences total shadowing effect: could make effective σ_{abs} without shadowing depend on y , $\sqrt{S_{NN}}$

Feed down to J/ψ from χ_c and ψ' decays included

$$\sigma_{pA} = \sigma_{pN} \int d^2b [0.6S_{\psi, \text{dir}}(b) + 0.3S_{\chi_{cJ}}(b) + 0.1S_{\psi'}(b)]$$

Comparing Absorption Calculations

A^α with $\alpha = 1 - 9\sigma_{\text{abs}}/(16\pi r_0^2)$, $\sigma_{\text{abs}} = 4.8$ mb is line on semi-log plot

Exponential survival probability with $S \propto \exp(-\rho_0\sigma_{\text{abs}}L)$ has convex shape. Using $\rho_0 = 0.16$ fm $^{-3}$ and $L = (3/4)r_0A^{1/3}$ gives smooth curve.

Real nuclear shapes (points) show fluctuations due to different densities, sizes

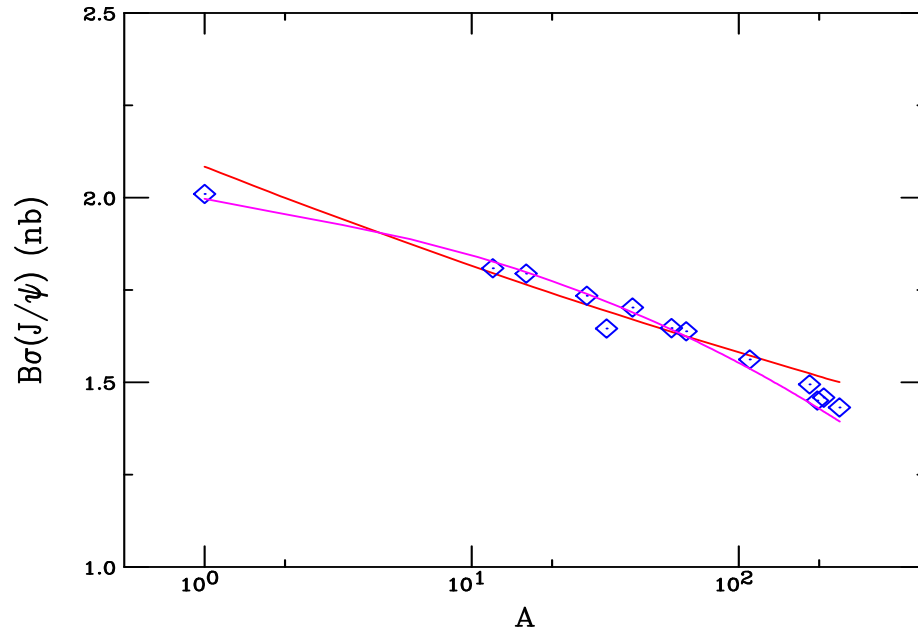


Figure 3: The J/ψ A dependence, all with $\sigma_{\text{abs}} = 4.8$ mb, normalized to typical SPS J/ψ cross section. The red line is the result for A^α , the dashed with $\exp(-\rho_0\sigma_{\text{abs}}L)$ and the points are numerical calculations of the survival probability with real nuclear shapes.

A Dependence of J/ψ and ψ' Not Identical

Color octet mechanism suggested that J/ψ and ψ' A dependence should be identical — Supported by large uncertainties of early data

More extensive data sets (NA50 at SPS, E866 at FNAL) show clear difference at midrapidity [NA50 ρL fit gives $\Delta\sigma = \sigma_{\text{abs}}^{\psi'} - \sigma_{\text{abs}}^{J/\psi} = 4.2 \pm 1.0$ mb at 400 GeV, 2.8 ± 0.5 mb at 450 GeV for absolute cross sections]

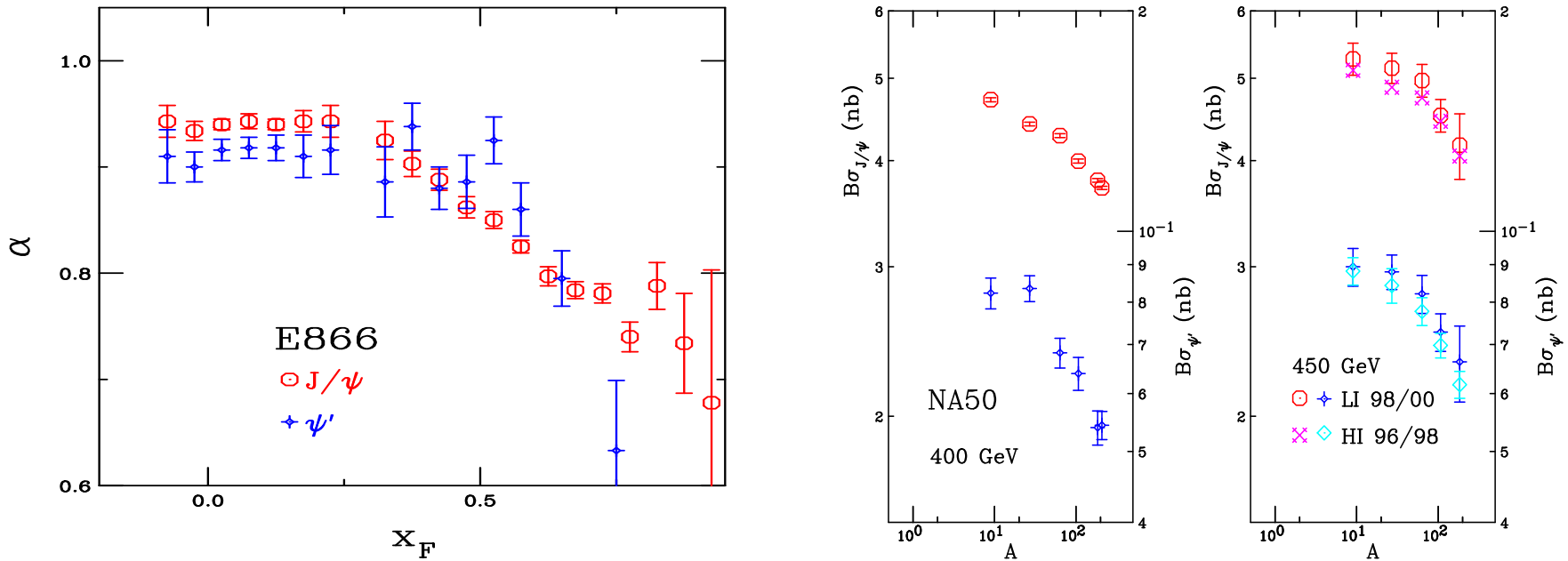


Figure 4: The J/ψ A dependence (left) as a function of x_F at FNAL ($\sqrt{s_{NN}} = 38.8$ GeV) and (right) and a function of A at the SPS (NA50 at $p_{\text{lab}} = 400$ and 450 GeV) for J/ψ and ψ' production.

Nuclear Absorption Calculations

Assume that each charmonium state interacts with a different constant asymptotic absorption cross section

$$\sigma_{\text{abs}}^C = \sigma_{\text{abs}}^{J/\psi} \left(\frac{r_C}{r_{J/\psi}} \right)^2$$

The χ_c A dependence remains unknown

We take $r_{\chi_c} = 1.44 r_{J/\psi}$ and $r_{\psi'} = 1.8 r_{J/\psi}$ (Satz)

Measurements from SPS to RHIC suggest that absorption decreases with increasing energy while shadowing effects increase

Predictions that quarkonium absorption cross sections decrease with energy agree with trend of data (M. A. Braun *et al.*, Nucl. Phys. B 509 (1998) 357 [hep-ph/9707424], A. Capella and E. G. Ferreira, hep-ph/0610313)

Absorption alone always gives less than linear A dependence ($\alpha < 1$)

Interplay of Shadowing and Absorption

Depending on x values probed, shadowing can enhance or reduce absorption cross section needed to describe data

For SPS energies, $17.3 \leq \sqrt{S} \leq 29$ GeV, rapidity range covered is in EMC and antishadowing region, $\alpha > 1$ with no absorption

Adding shadowing to absorption calculations here means a larger absorption cross section is needed to maintain agreement with data

For $\sqrt{S} \geq 38$ GeV, x in shadowing regime, thus $\alpha < 1$ with shadowing alone in forward region, reducing needed absorption cross section

Shadowing and Absorption at the SPS: A Dependence

Stronger antishadowing of EKS98 in SPS midrapidity region calls for bigger absorption cross section

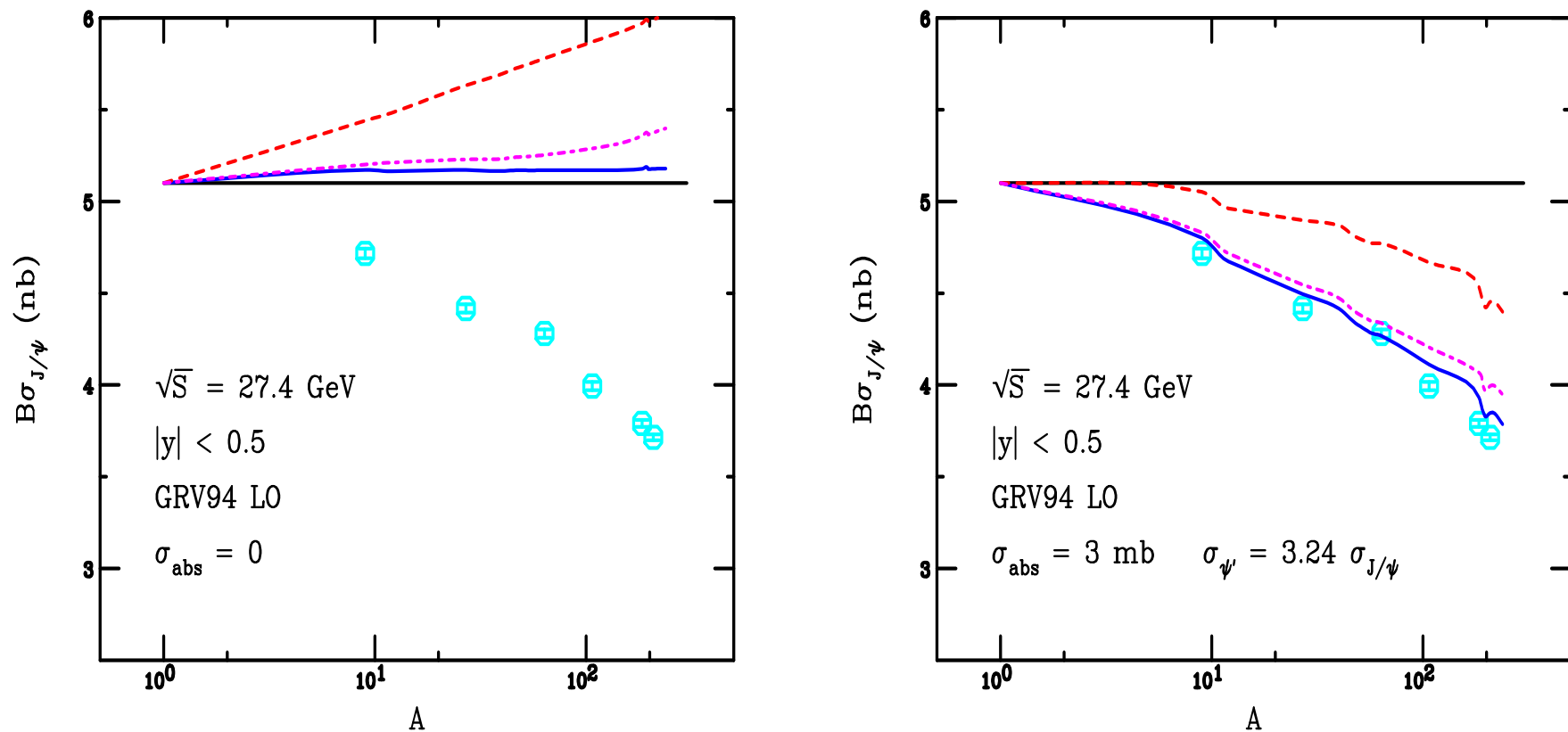


Figure 5: The J/ψ A dependence at 400 GeV for no absorption (left) and for $\sigma_{\text{abs}}^{J/\psi} = 3$ mb (right). The curves are with no shadowing (solid blue), EKS98 (magenta dot-dashed) and nDSg (red dashed).

Shadowing and Absorption at the SPS: y Dependence

Rapidity dependence becomes more pronounced with increasing A
 Order of R_{pA} per nucleon reversed when absorption added

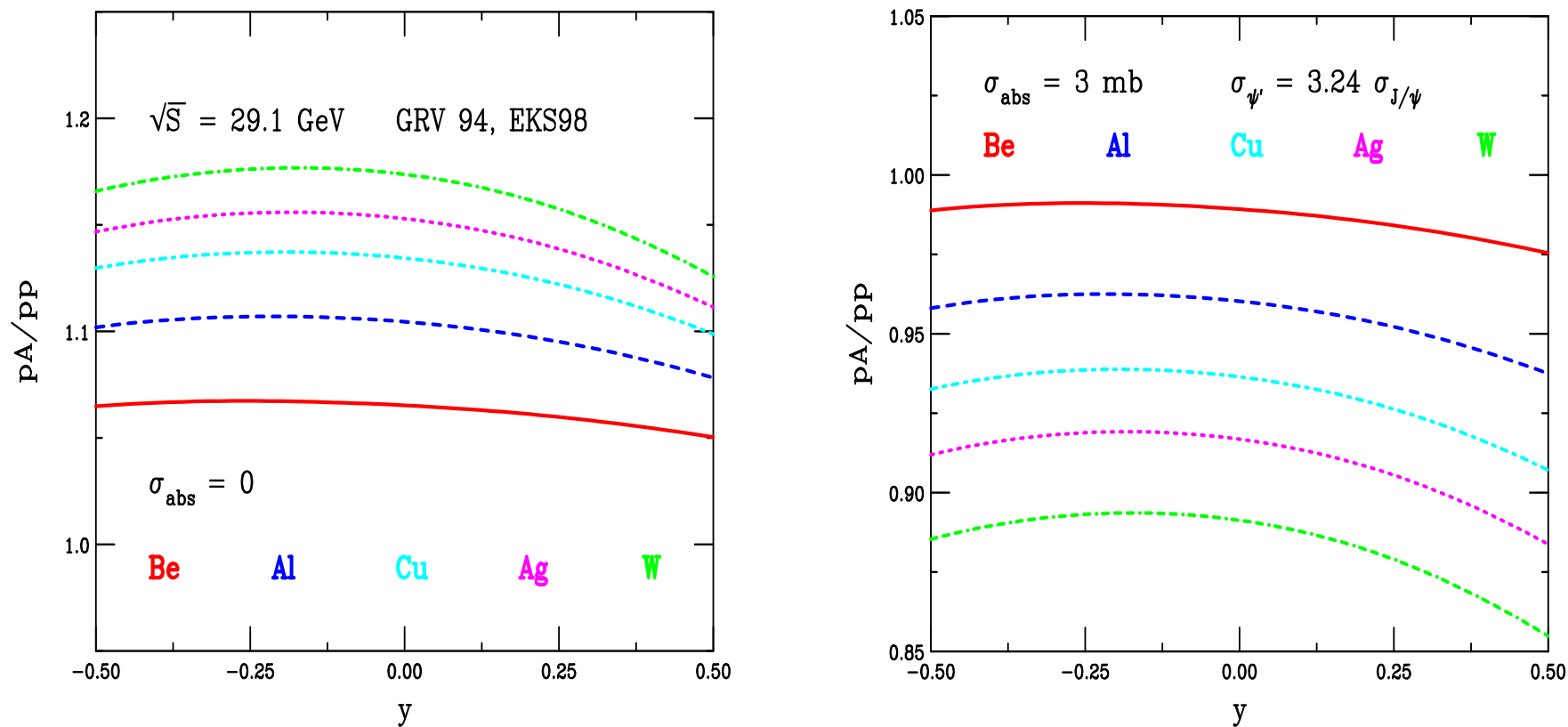


Figure 6: The J/ψ A dependence at 400 GeV for no absorption (left) and for $\sigma_{\text{abs}}^{J/\psi} = 3$ mb (right) with the GRV 94 parton densities and EKS98 shadowing parameterization.

Shadowing and Absorption at the SPS: PDF

y dependence can discriminate PDF and shadowing parameterization
 Difference in shape between GRV and MRST/CTEQ due to smaller scale used in GRV calculation

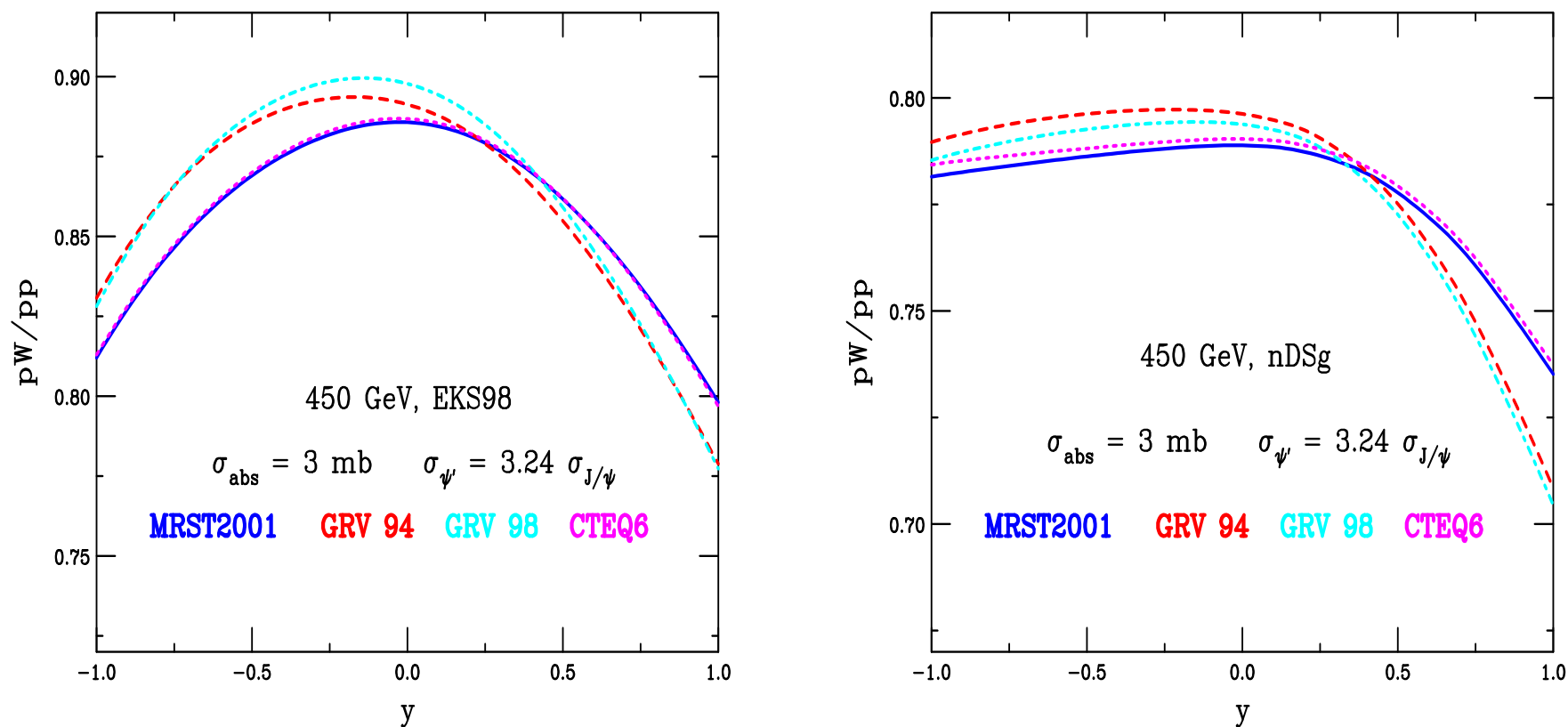


Figure 7: The J/ψ y dependence at 450 GeV for EKS98 (left) and nDSg (right) with $\sigma_{\text{abs}}^{J/\psi} = 3 \text{ mb}$.

Fitting the J/ψ and ψ' Absorption Cross Sections: I

Using single absorption cross section for J/ψ and ψ' give quite different absorption cross sections at SPS energies

GRV 94 results shown, similar results for GRV 98, MRST2001 and CTEQ6

J/ψ					ψ'				
Shadowing	Data	$B\sigma_0(400)$ (nb)	$B\sigma_0(450)$ (nb)	$\sigma_{\text{abs}}^{J/\psi}$ (mb)	Shadowing	Data	$B\sigma_0(400)$ (nb)	$B\sigma_0(450)$ (nb)	$\sigma_{\text{abs}}^{\psi'}$ (mb)
no shad.	400 GeV	5.02	-	4.65	no shad.	400 GeV	102.1	-	10.66
	HI 96/98	-	5.49	4.57		HI 96/98	-	101.8	8.12
	LI 98/00	-	5.67	4.26		LI 98/00	-	101.6	6.45
	combined	5.02	5.60	4.67		combined	98.2	108.7	9.56
EKS98	400 GeV	4.97	-	7.02	EKS98	400 GeV	101.2	-	13.58
	HI 96/98	-	5.41	6.87		HI 96/98	-	100.5	10.74
	LI 98/00	-	5.58	6.52		LI 98/00	-	100.6	9.05
	combined	4.96	5.52	6.99		combined	99.0	109.5	12.90
nDSg	400 GeV	5.05	-	5.23	nDSg	400 GeV	100.5	-	10.74
	HI 96/98	-	5.52	5.11		HI 96/98	-	102.5	8.76
	LI 98/00	-	5.69	4.70		LI 98/00	-	101.9	6.90
	combined	5.04	5.61	5.19		combined	99.0	109.8	10.31

Figure 8: The values of $B\sigma_0$ at 400 GeV and 450 GeV and the absorption cross section, σ_{abs} , found by fitting the NA50 J/ψ (left) and ψ' (right) cross section data with a single absorption cross section for J/ψ , ψ' and χ_c with the GRV94 PDFs without shadowing and with EKS98 and nDSg shadowing parameterizations.

Fitting the J/ψ and ψ' Absorption Cross Sections: II

Using feeddown with different asymptotic cross sections gives similar J/ψ absorption cross section from fits to J/ψ and ψ' data

GRV 98 results shown, similar results for GRV 94, MRST2001 and CTEQ6

J/ψ					ψ'				
Shadowing	Data	$B\sigma_0(400)$ (nb)	$B\sigma_0(450)$ (nb)	$\sigma_{\text{abs}}^{J/\psi}$ (mb)	Shadowing	Data	$B\sigma_0(400)$ (nb)	$B\sigma_0(450)$ (nb)	$\sigma_{\text{abs}}^{J/\psi}$ (mb)
no shad.	400 GeV	5.04	-	3.15	no shad.	400 GeV	101.1	-	3.18
	HI 96/98	-	5.53	3.15		HI 96/98	-	100.9	2.41
	LI 98/00	-	5.70	2.89		LI 98/00	-	103.0	2.10
	450 GeV	-	5.64	3.20		450 GeV	-	101.4	2.31
	combined	5.03	5.61	3.14		combined	99.2	109.6	3.01
EKS98	400 GeV	4.99	-	4.98	EKS98	400 GeV	100.6	-	4.17
	HI 96/98	-	5.37	4.61		HI 96/98	-	96.7	3.00
	LI 98/00	-	5.61	4.61		LI 98/00	-	102.2	2.99
	450 GeV	-	5.46	4.61		450 GeV	-	100.8	3.23
	combined	4.99	5.56	4.99		combined	98.6	108.7	3.98
nDSg	400 GeV	5.10	-	3.65	nDSg	400 GeV	100.9	-	3.31
	HI 96/98	-	5.50	3.31		HI 96/98	-	101.2	2.56
	LI 98/00	-	5.71	3.16		LI 98/00	-	103.7	2.27
	450 GeV	-	5.59	3.31		450 GeV	-	101.8	2.47
	combined	5.09	5.68	3.64		combined	99.8	110.5	3.22

Figure 9: The values of $B\sigma_0$ at 400 GeV and 450 GeV and the absorption cross section, σ_{abs} , found by fitting the NA50 J/ψ (left) and ψ' (right) cross section data with different absorption cross sections for J/ψ , ψ' and χ_c assuming that $\sigma_{\text{abs}}^{\psi'} = 3.24\sigma_{\text{abs}}^{J/\psi}$ with the GRV98 PDFs without shadowing and with EKS98 and nDSg shadowing parameterizations.

Fitting the J/ψ and ψ' Absorption Cross Sections: III

While absolute absorption cross sections different, fits are all similarly 'good'

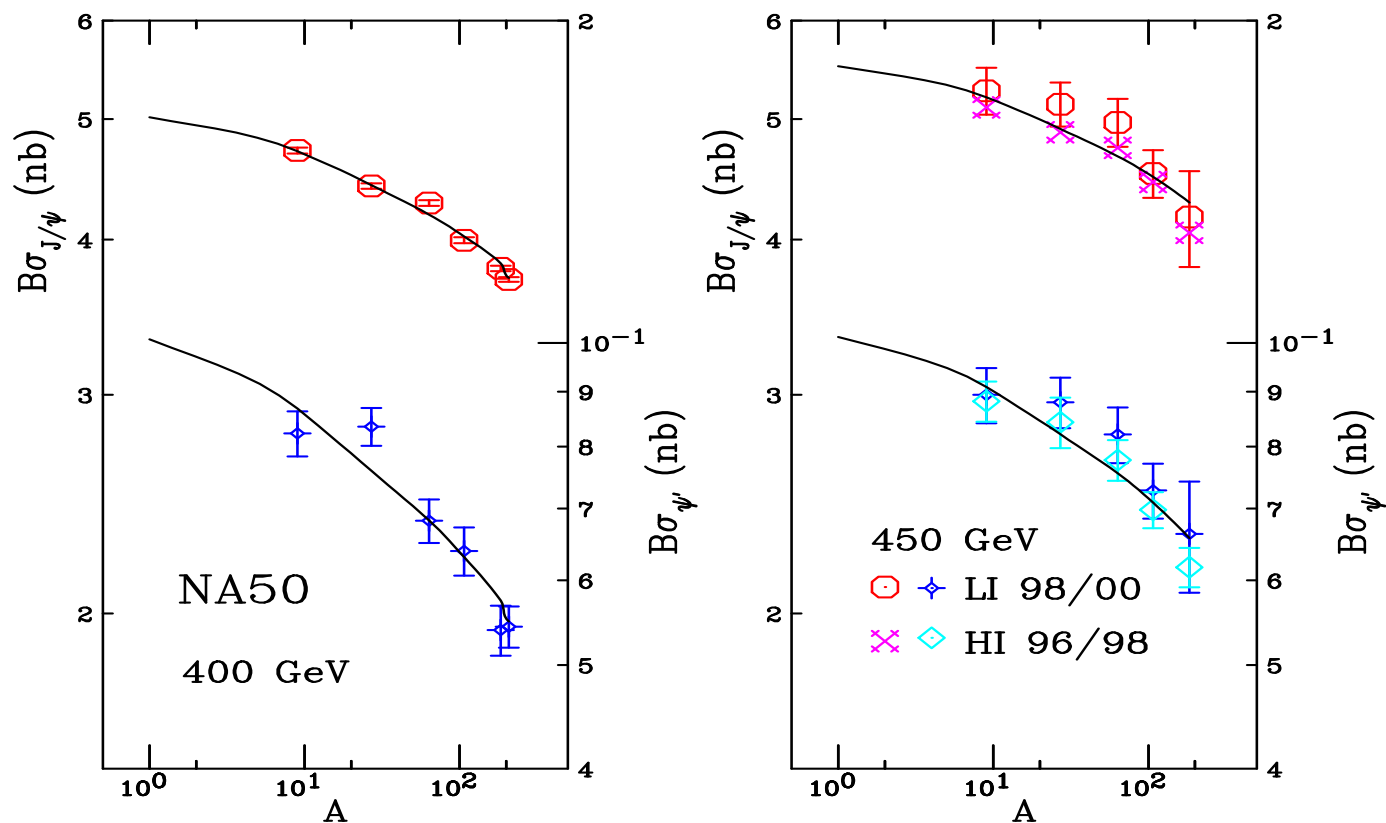


Figure 10: The J/ψ A dependence at 400 (left) and 450 (right) GeV.

Shadowing and Absorption at the SPS: σ_{abs} Dependence

pA/pp ratio decreases incrementally with increasing σ_{abs}

Shape of rapidity distribution unchanged by increasing absorption

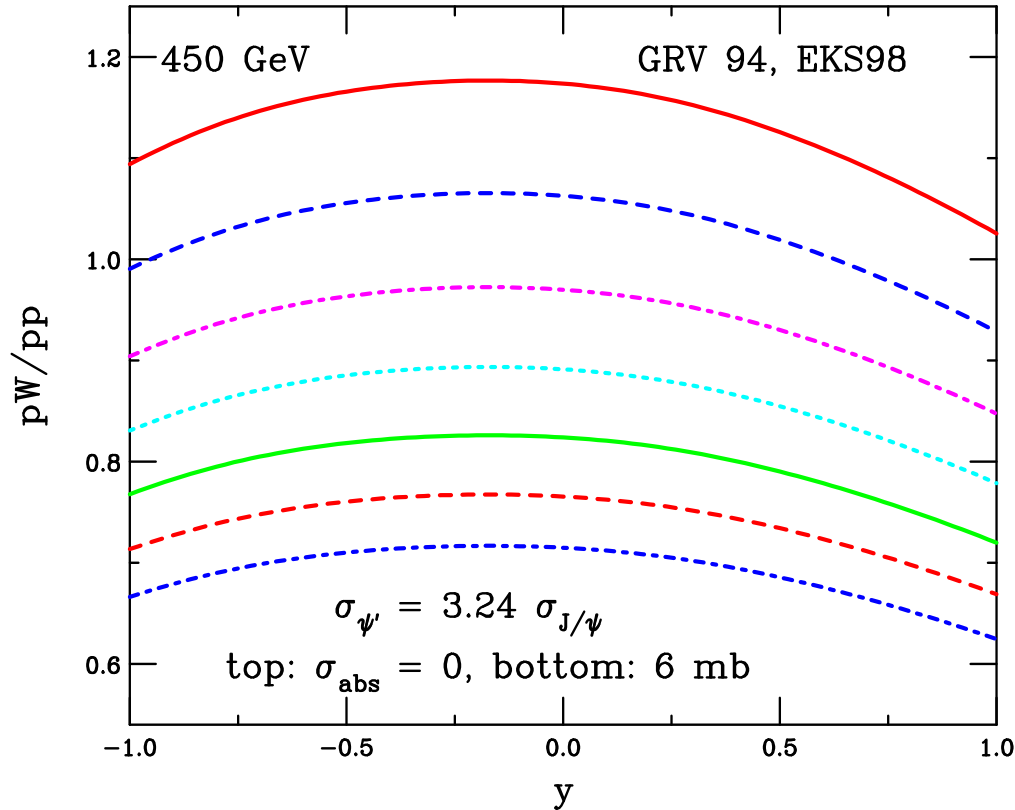


Figure 11: The J/ψ y dependence at 450 GeV for increasing σ_{abs} by 1 mb with the GRV 94 parton densities and EKS98 shadowing parameterization.

Predicted J/ψ Rapidity Distributions at RHIC

Agreement of color evaporation model (CEM) with overall normalization of PHENIX data good

Shape has right trend for d+Au with EKS98 shadowing

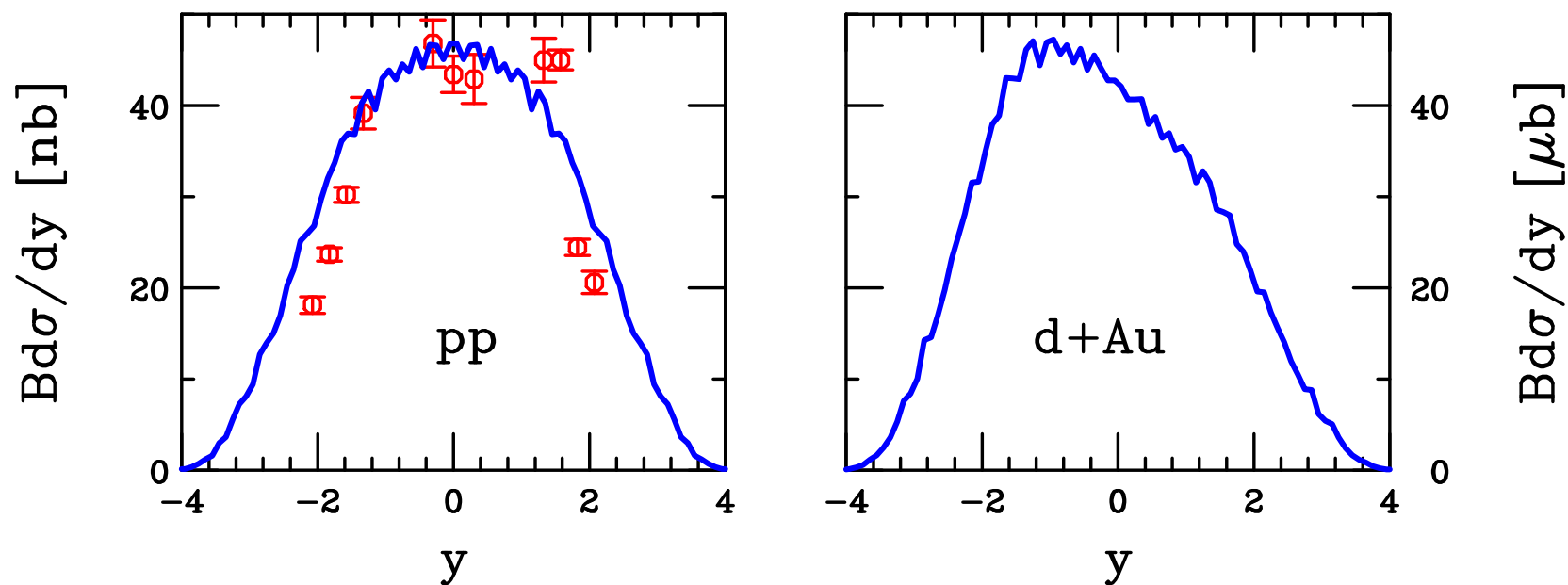


Figure 12: The inclusive J/ψ y distributions in $\sqrt{S} = 200$ GeV pp interactions (left-hand side) calculated with the MRST parton densities in the CEM with $m_c = 1.2$ GeV, $\mu = 2m_T$. The rapidity distribution for d+Au collisions (right-hand side with EKS98) is also shown.

Absorption and Shadowing at RHIC: $R_{dAu}(y)$

Feeddown from higher states with larger absorption cross sections needs $\sigma_{\text{abs}}^{J/\psi} < 2 \text{ mb}$ with present d+Au data

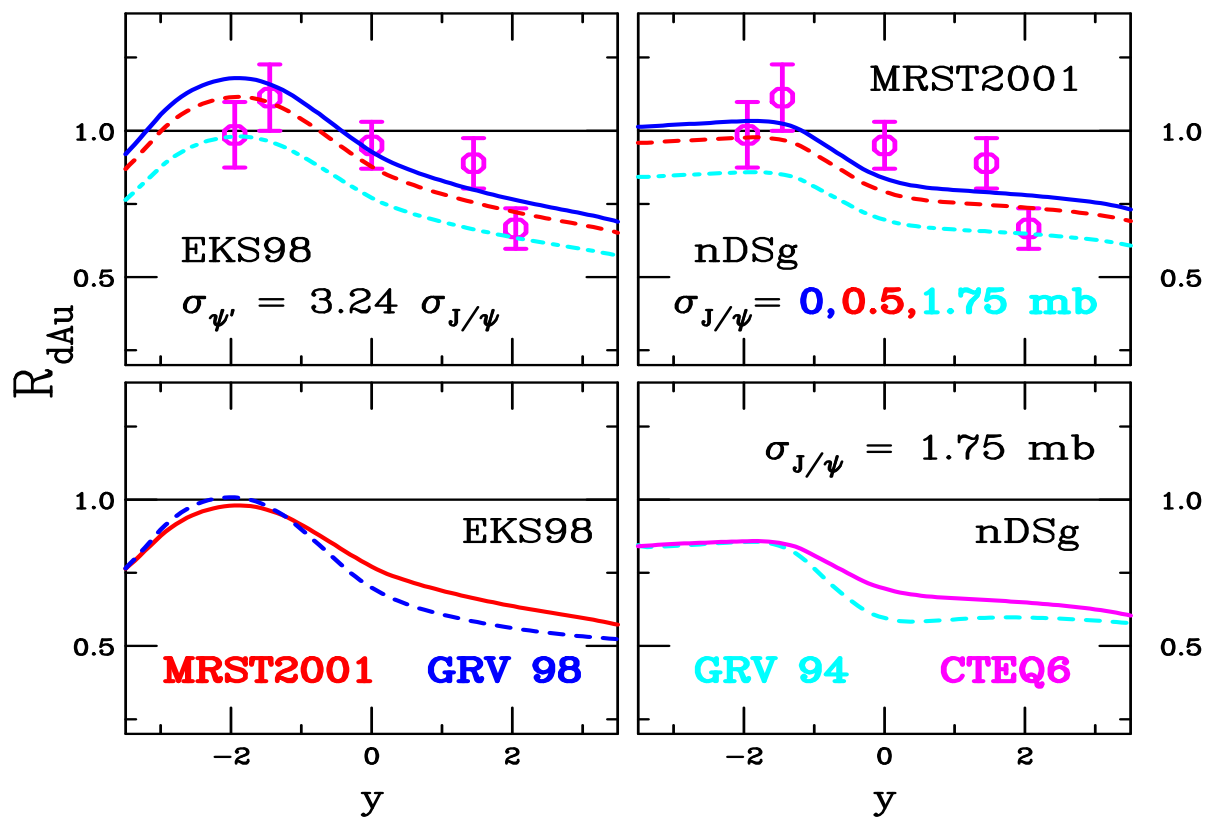


Figure 13: The d+Au/pp ratio as a function of rapidity for EKS98 (left) and nDSg (right) parameterizations. The top plots vary the J/ψ absorption cross section with the MRST2001 PDFs while the bottom plots show the differences in the PDF choice for a fixed absorption cross section.

Absorption and Shadowing at RHIC: $R_{\text{AuAu}}(y)$

R_{AA} rather flat with rapidity, agreement with data for $\sigma_{\text{abs}}^{J/\psi} \sim 1 \text{ mb}$

Convolution of shadowing parameterizations give dip at midrapidity

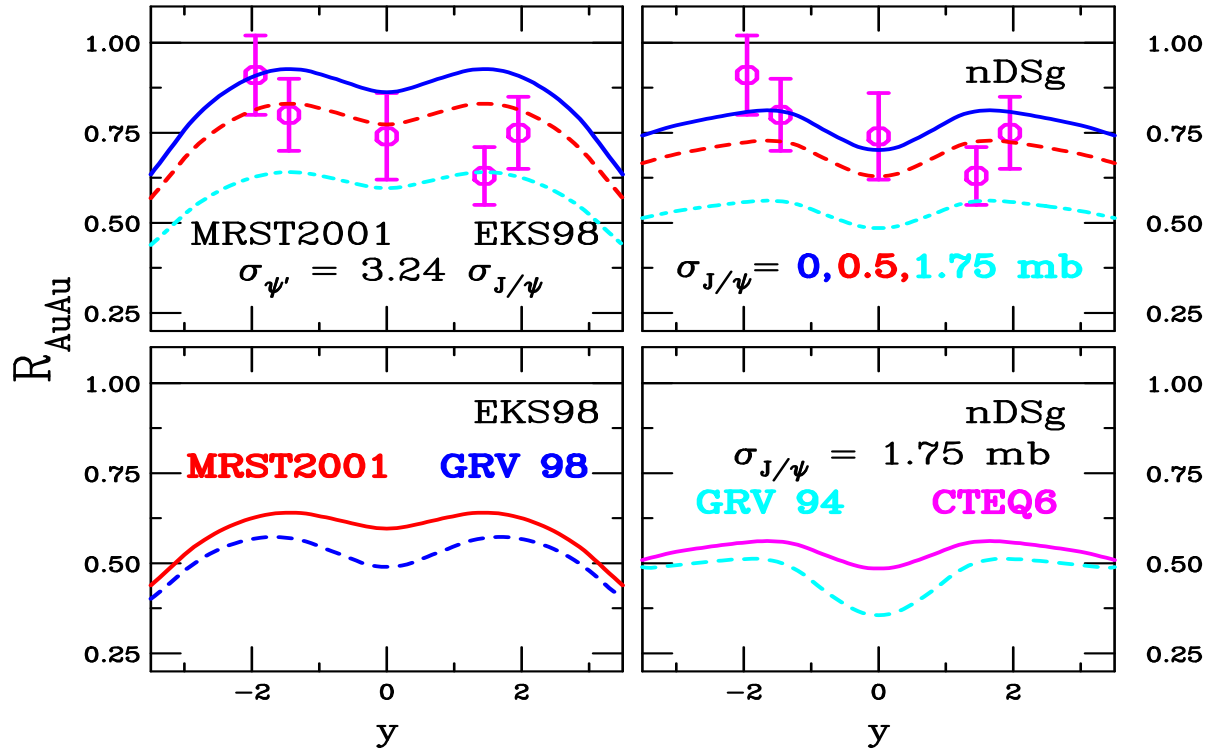


Figure 14: The AuAu/ pp ratio as a function of rapidity for EKS98 (left) and nDSg (right) parameterizations. The top plots vary the J/ψ absorption cross section with the MRST2001 PDFs while the bottom plots show the differences in the PDF choice for a fixed absorption cross section. The PHENIX data in the 60-90% centrality bin are shown.

Absorption and Shadowing at RHIC: $R_{\text{CuCu}}(y)$

Shadowing reduced for Cu relative to Au

Lower energy Cu+Cu probes larger x , EKS98 antishadowing peaks coincide at midrapidity

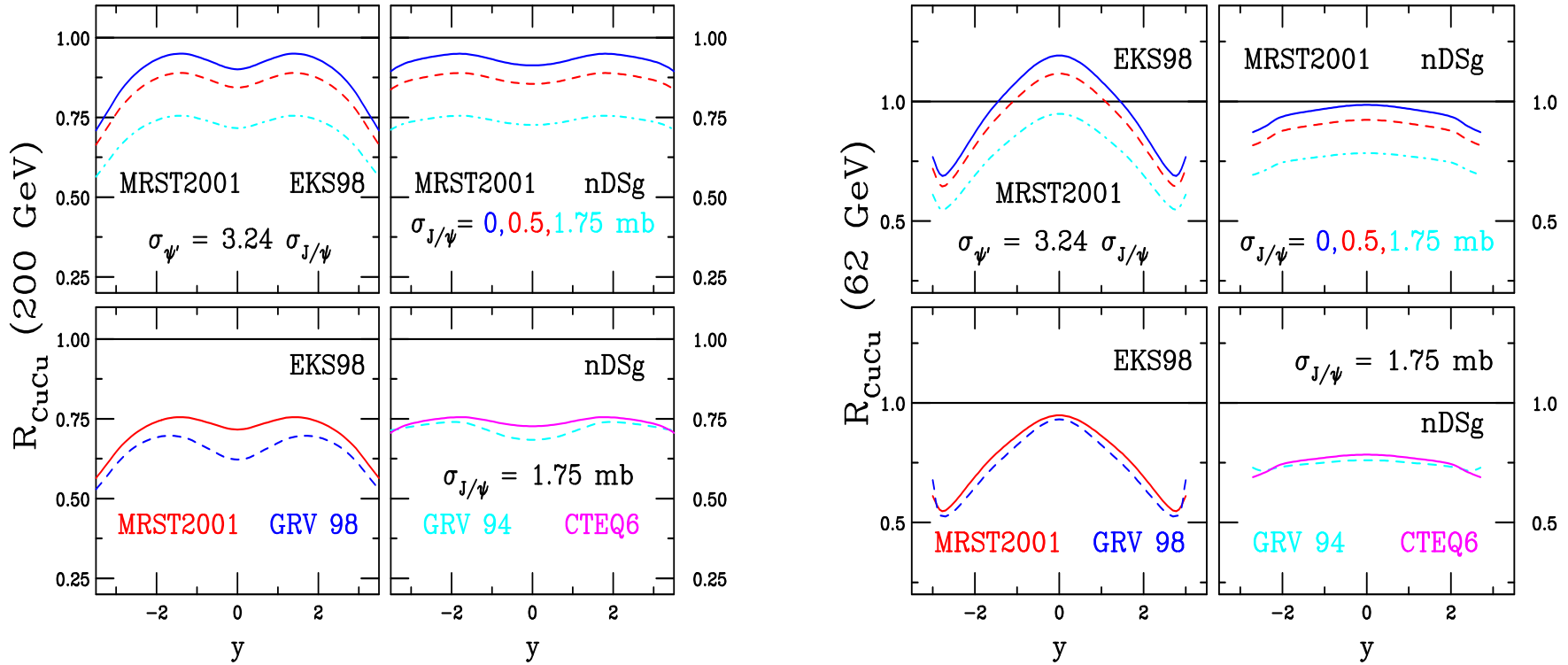


Figure 15: The CuCu/ pp ratio as a function of rapidity for EKS98 (left) and nDSg (right) parameterizations. The top plots vary the J/ψ absorption cross section with the MRST2001 PDFs while the bottom plots show the differences in the PDF choice for a fixed absorption cross section.

Centrality Dependence of Shadowing and Absorption

PHENIX d+Au results presented as a function of the number of binary nucleon-nucleon collisions, N_{coll} , the convolution of the nuclear profile functions multiplied by the inelastic NN cross section, 42 mb at RHIC

$$N_{\text{coll}}(b) = \sigma_{NN}^{\text{in}} \int d^2s T_A(s) T_B(|\vec{b} - \vec{s}|)$$

AA results presented as a function of the number of nucleon participants, N_{part} ,

$$N_{\text{part}}(b) = \int d^2s [T_A(s)(1 - \exp(-\sigma_{NN} T_B(|\vec{b} - \vec{s}|))) + T_B(|\vec{b} - \vec{s}|)(1 - \exp(-\sigma_{NN} T_A(s)))]$$

Results with EKS98 and nDSg compared at $y = -1.7$ (antishadowing), 0 (transition region) 1.7 (shadowing)

Absorption and Shadowing at RHIC: $R_{dAu}(N_{\text{coll}})$

Largest difference between shadowing parameterizations is in anti-shadowing region ($y = -1.7$), PDF difference is not large

Data do not strongly distinguish between different σ_{abs}

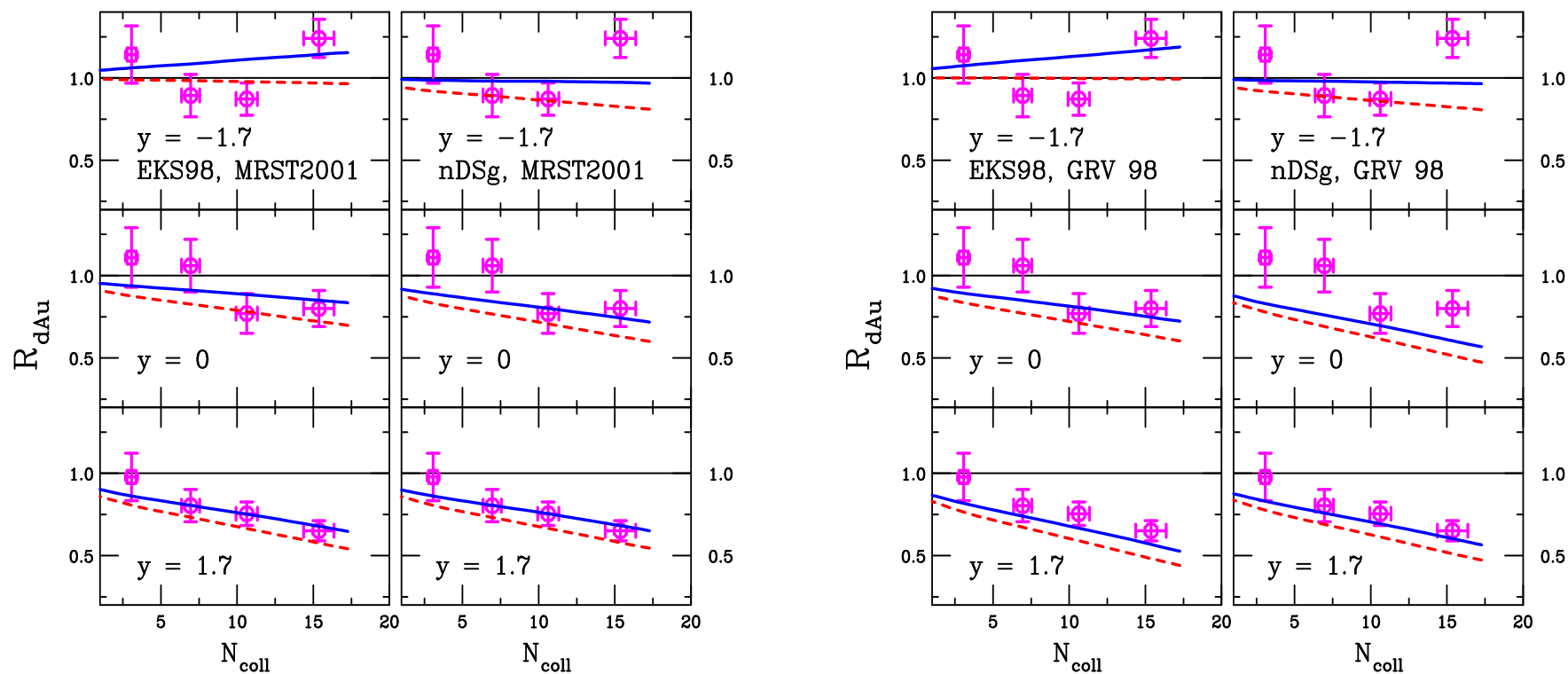


Figure 16: The dAu/pp ratio as a function of the number of collisions calculated with EKS98 (left) and nDSg (right) on each plot with the MRST2001 (left-hand plot) and GRV 98 (right-hand plot) PDFs. The curves are for $\sigma_{\text{abs}}^{J/\psi} = 0.5$ (solid blue) and 1.75 mb (dashed red). PHENIX data are shown for d+Au collisions at 200 GeV for $y = -1.7$ (top), 0 (middle) and 1.7 (bottom). (An additional 12% overall normalization error is not shown.)

Absorption and Shadowing at RHIC: $R_{\text{AuAu}}(N_{\text{part}})$

Cold matter effects with $\sigma_{\text{abs}} \sim 1$ mb in relatively good agreement with midrapidity data

Stronger N_{part} dependence at forward rapidity than predicted

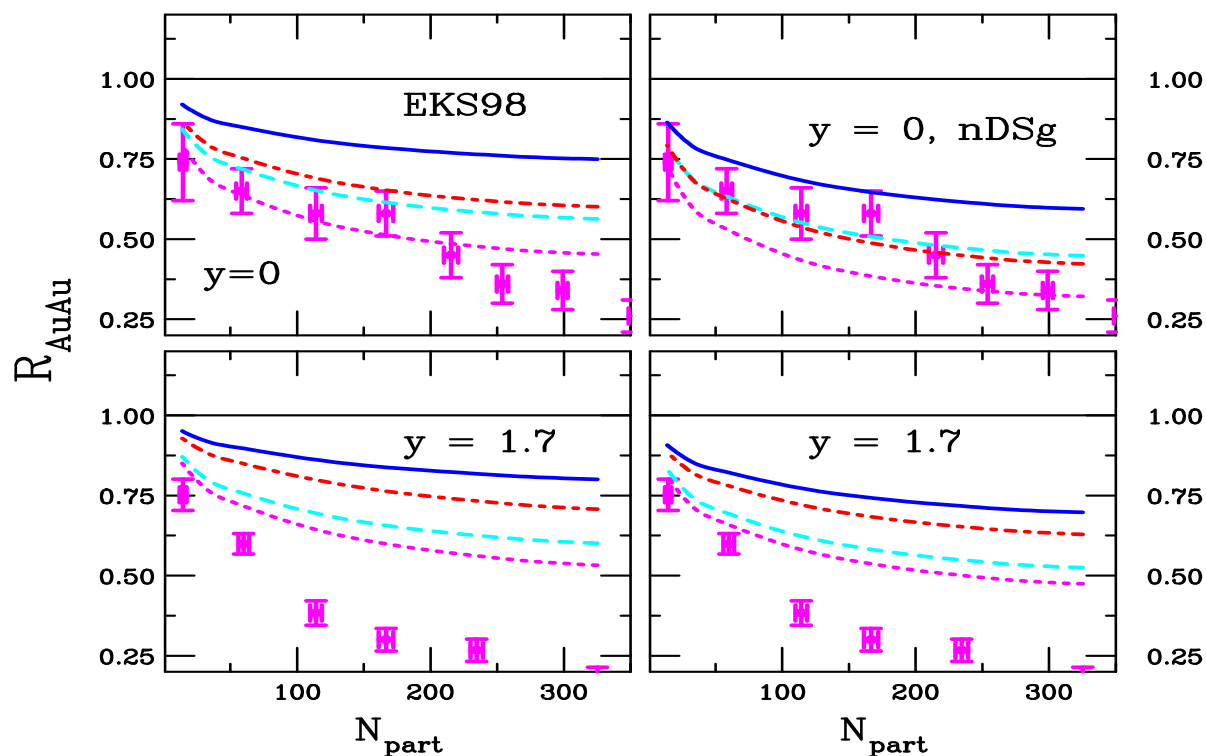


Figure 17: The AuAu/pp ratio as a function of the number of participants calculated with EKS98 (left) and nDSg (right). The curves are for $\sigma_{\text{abs}}^{J/\psi} = 0.5$ (dashed cyan - MRST2001 and dot-dashed red - GRV 98) and 1.75 mb (solid blue - MRST2001 and dotted magenta - GRV 98). PHENIX data are shown for Au+Au collisions at 200 GeV for $y = 0$ (top), and 1.7 (bottom).

Absorption and Shadowing at RHIC: $R_{\text{CuCu}}(N_{\text{part}})$

Forward results for both energies similar while differences seen at midrapidity

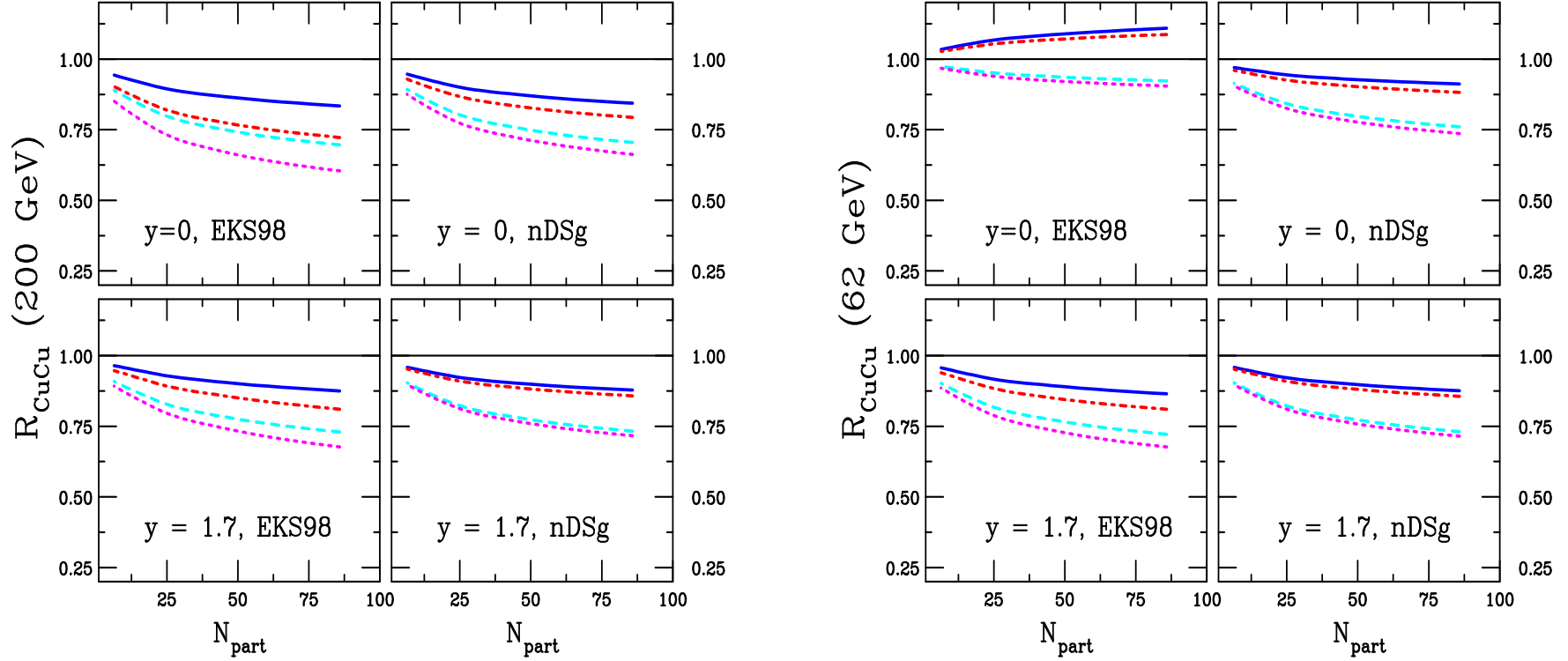


Figure 18: The CuCu/pp ratio as a function of the number of participants for $\sqrt{S_{NN}} = 200$ (left-hand plot) and 62 (right-hand plot) GeV, calculated with EKS98 (left) and nDSg (right) on each plot. The curves are for $\sigma_{\text{abs}}^{J/\psi} = 0.5$ (dashed cyan - MRST2001 and dot-dashed red - GRV 98) and 1.75 mb (solid blue - MRST2001 and dotted magenta - GRV 98).

Summary .

- Data clearly show that J/ψ and ψ' have different A dependence, translates into different effective absorption for J/ψ and ψ'
- SPS shadowing and absorption calculations show larger absorption cross sections needed to counter antishadowing effects but $\sigma_{\text{abs}}^{J/\psi}$ smaller overall if $\sigma_{\text{abs}}^{\psi'} > \sigma_{\text{abs}}^{J/\psi}$
- Measurement of χ_c A dependence would provide additional test of absorption mechanism
- Current d+Au J/ψ data agree well with combination of initial state shadowing and final state absorption
- Data seem to suggest absorption cross section decreases with $\sqrt{S_{NN}}$
- Need better statistics to distinguish between shadowing parameterizations and determine strength of absorption at RHIC
- Cold matter effects need to be accounted for in AA collisions but room for dense matter effects